In situ observation of transformation in α-Fe_2O_3 under hydrogen implantation

2002 J. Phys.: Condens. Matter 14 13643

(http://iopscience.iop.org/0953-8984/14/49/318)

INSTITUTE OF PHYSICS PUBLISHING JOURNAL OF PHYSICS: CONDENSED MATTER

J. Phys.: Condens. Matter **14** (2002) 13643–13651 PII: S0953-8984(02)38377-2

In situ observation of transformation in α-Fe_2O_3 under hydrogen implantation

Yoshimi Watanabe[1,5], Kuniyoshi Ishii[2], Nobuhiro Ishikawa[3], Kazuo Furuya[3] and Masaharu Kato[4]

[1] Department of Functional Machinery and Mechanics, Shinshu University, 3-15-1, Tokida, Ueda 386-8567, Japan
[2] Division of Materials Science and Engineering, Hokkaido University, N-13, W-8, Kita-ku, Sapporo 060-8628, Japan
[3] Materials Engineering Laboratory, National Institute for Materials Science, Sengen 1-2-1, Tsukuba-shi, Ibaraki 305-0047, Japan
[4] Department of Innovative and Engineered Materials, Tokyo Institute of Technology, 4259 Nagatsuta, Midori-ku, Yokohama 226-8502, Japan

E-mail: yoshimi@giptc.shinshu-u.ac.jp

Received 19 June 2002
Published 29 November 2002
Online at stacks.iop.org/JPhysCM/14/13643

Abstract

An *in situ* observation of the α-Fe_2O_3-to-Fe_3O_4 transformation has been performed using a dual-ion-beam accelerator interfaced with a transmission electron microscope (TEM). During the hydrogen-ion implantation of α-Fe_2O_3, transformation into the new phase (γ-Fe_2O_3 or Fe_3O_4) was observed. It was also found that the orientation relationship between α-Fe_2O_3 and the new phase (γ-Fe_2O_3 or Fe_3O_4) satisfies the Shoji–Nishiyama relationship, in agreement with previous experiments. It was also found that the nearest interatomic distance does not vary by the implantation until the re-stacked phase appears, although when the re-stacked phase is formed, the lattice expansion is observed in the transformed (re-stacked) phase. Judging from these results, we have concluded that the α-Fe_2O_3 to Fe_3O_4 transformation is induced during the hydrogen ion implantation of α-Fe_2O_3.

1. Introduction

There are various iron oxides, e.g., α-Fe_2O_3 (haematite), γ-Fe_2O_3 (maghemite), Fe_3O_4 (magnetite) and $Fe_{1-x}O$ (wustite). It is well known that different iron oxides can be transformed into others by reduction or oxidation reactions [1–3]. Examinations of these transformations in iron oxides are generally performed by observing post-reduction or post-oxidation samples, i.e., *ex situ* examinations by optical, scanning and transmission electron microscopy (TEM). Such conventional studies, however, have a disadvantage, since structural changes may occur when the specimen is cooled and transferred to the microscope. The alternative to *ex situ*

[5] Author to whom any correspondence should be addressed.

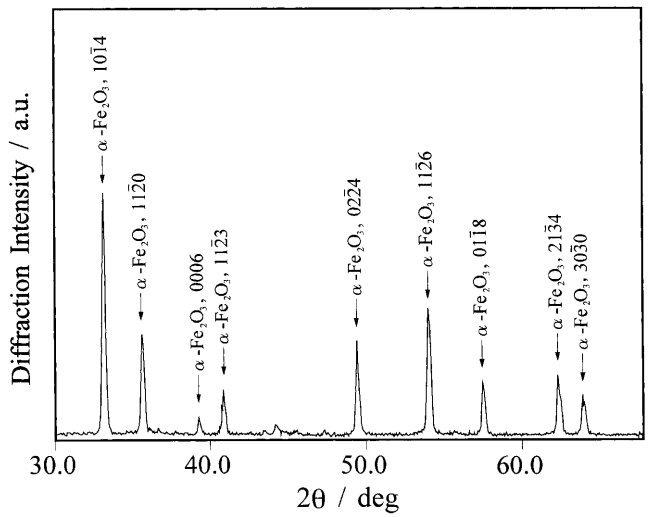

Figure 1. The x-ray diffraction pattern showing the presence of α-Fe_2O_3.

examinations is the use of an 'environmental cell' within the TEM [4, 5] or a hot-stage environmental scanning microscope [6–8].

Ion implantation is a unique method for implanting atoms and creating metastable phases without any thermodynamical restrictions. In a recent study, Watanabe *et al* [9] found that the transformation from α-Fe_2O_3 to Fe_3O_4 was induced in a hydrogen implantation experiment in which the specimens were implanted outside the TEM. Since the orientation relationship obtained by the hydrogen implantation experiment was in agreement with those of previous studies [4, 6], it was concluded that information concerning microstructural changes during the transformation could be obtained from this experiment.

In situ ion implantation during observation in a TEM is one of the fascinating methods available for investigating the structural evolutions of materials induced by the particle implantation [10–13]. This paper reports the results of the *in situ* observation of the α-Fe_2O_3-to-Fe_3O_4 transformation induced by hydrogen-ion implantation, using a TEM with a dual-ion-beam interface [13]. Using the experimental results, the validity of the transformation model proposed by Watanabe and Ishii [14] will be discussed.

2. Experimental procedures

2.1. Sample preparation

The α-Fe_2O_3 specimens used in the present study were taken from the natural dense haematite ore, MBR (Mineracoes Brasileiras Reunidas) ore, originating in Brazil. The chemical composition of the ore is Fe_2O_3: 97.04, FeO: 0.34, SiO_2: 0.83, Al_2O_3: 0.45, CaO: 0.14, MgO: 0.05 (in mass per cent). The amount of gangue (sums of the mass percentages of SiO_2, Al_2O_3, CaO and MgO) in the MBR ore is known to be smaller than in any other α-Fe_2O_3 ore, such as the Mount Newman ore or the Itabira ore. For eliminating possible influences of the impurities on the transformation, the MBR ore is considered to be best suited.

Figure 1 shows the x-ray diffraction pattern of the MBR ore. As can be seen from this figure, all observable peaks are those of α-Fe_2O_3, and no evidence for the presence of other phases such as Fe_3O_4 is found. In this way, the MBR ore, used in this study, was identified as consisting of single-phase α-Fe_2O_3.

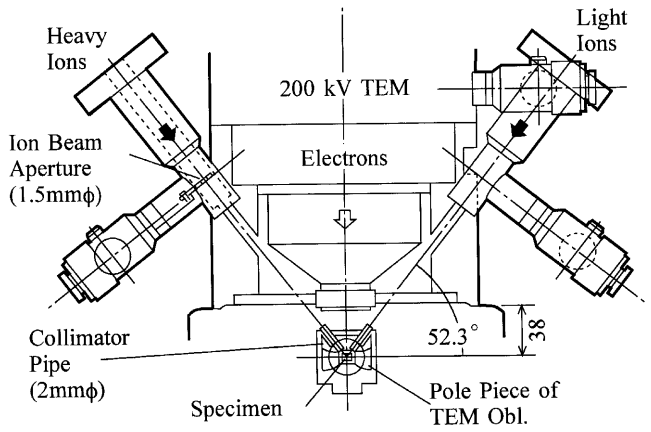

Figure 2. Schematic drawing of the *in situ* implantation facility based on a 200 keV TEM with dual ion beam accelerator [13].

Specimens of α-Fe_2O_3 were prepared by grinding and polishing to a thickness of approximately 30 μm from cleavage-fractured pieces. Then, specimens were bonded with stainless steel rings to reinforce them, since the MBR ore is very brittle. Final thinning was done by means of an ion mill.

2.2. In situ hydrogen implantation

The present *in situ* implantation study was carried out in a 200 kV TEM (200Fx) with a dual-ion-beam interface at the Materials Engineering Laboratory, National Institute for Materials Science. Figure 2 shows the schematic drawing of the 2000FX with a dual ion beam interface, for which a detailed description was given by Ishikawa and Furuya [13]. In this study, hydrogen is used to trigger the transformation, since hydrogen is a reducing gas. Hydrogen was implanted as H^+ at room temperature by using the light-ion source of the dual-ion-beam interface. The depth distribution of the implanted hydrogen ions can be controlled by the implantation energy, and the depth profiles were calculated by the TRIM code [15]. Although no data are presented here, it was found that all implanted ions stay within the specimen when the specimen is implanted with 20 keV H^+ ions. The ion-beam profile was examined by a Faraday cup placed at the specimen position.

Since it is known that Fe_3O_4 grows with the close-packed (111) planes parallel to the basal (0001) planes of α-Fe_2O_3 [4, 9, 16], the (0001) planes of α-Fe_2O_3 were observed during the ion implantation. The crystallographic relationship between α-Fe_2O_3 and Fe_3O_4 was studied by means of electron diffraction.

3. Results

The microstructure (bright-field image) and the corresponding electron diffraction pattern of the specimen before hydrogen-ion implantation are shown in figures 3(a) and (b), respectively. The dark curved lines in the bright-field image are thickness fringes. One can see in these figures that only the α-Fe_2O_3 phase is found, and no reflection spots of the Fe_3O_4 phase can be seen before the implantation.

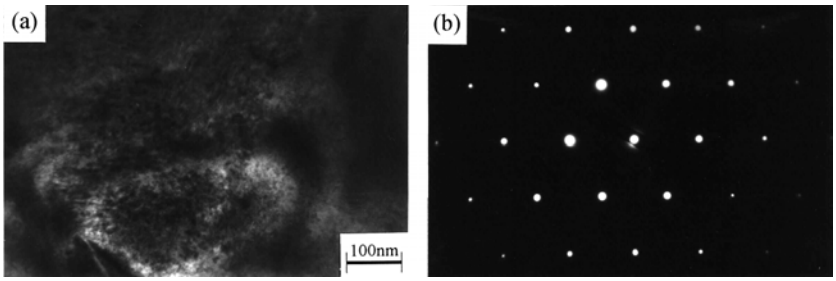

Figure 3. A transmission electron micrograph (a) and the electron diffraction pattern (b) of the sample before ion implantation. The sample is identified as single-phase α-Fe_2O_3 before ion implantation.

Figure 4 shows a sequence of microstructural changes induced by hydrogen-ion implantation. The total doses of (a)–(d) are 4.9×10^{19}, 4.13×10^{20}, 1.07×10^{21} and 2.26×10^{21} ions m^{-2}, respectively. Despite the fact that no notable change was observed in the bright-field images during the hydrogen-ion implantation, the diffraction patterns do show clear changes. As can be seen in figure 4(b), extra reflection spots in addition to the α-Fe_2O_3 spots exist.

The structural transformation of α-Fe_2O_3 to γ-Fe_2O_3 (maghemite) induced by hydrogen implantation is one possible explanation for the diffraction observations. Here, the crystal structure of γ-Fe_2O_3 is the same as that of Fe_3O_4 (that is, the crystal structure of γ-Fe_2O_3 resembles re-stacked α-Fe_2O_3) but γ-Fe_2O_3 has more vacancies in the iron sites compared to Fe_3O_4. γ-Fe_2O_3 exists as an ordered phase at low temperature and as a disordered cubic spinel at high temperatures [2, 17, 18]. However, we believe that there is another probable explanation for the observations presented here. The reduction reaction undergone by haematite under H+ implantation is probably to the Fe_3O_4 phase. γ-Fe_2O_3 and Fe_3O_4 are not distinguishable by means of electron diffraction (the lattice parameters and structure factors are nearly identical). Moreover, the same epitaxial orientation relationship for γ-Fe_2O_3/α-Fe_2O_3 is to be expected for Fe_3O_4/α-Fe_2O_3. The identification of a hydrogen-ion-implantation-induced phase will be discussed later.

These spots from the new phase (γ-Fe_2O_3 or Fe_3O_4) became stronger with increasing dose. These diffraction patterns can be indexed as the superposition of the $[0001]_h$ and $[111]_m$ diffraction patterns, as illustrated in figure 5. Here, the subscripts h and m denote α-Fe_2O_3 and γ-Fe_2O_3 or Fe_3O_4 crystals, respectively. The orientation relationship between α-Fe_2O_3 and γ-Fe_2O_3 or Fe_3O_4 is thus determined as

$$(0001)_h \parallel (111)_m, \qquad [100]_h \parallel [10]_m. \tag{1}$$

This may be called the well-known Shoji–Nishiyama orientation relationship [19, 20] between fcc and hcp crystals, in agreement with previous experiments [4, 9, 16, 21]. The reason that the new phase was detected only by means of diffraction patterns and not bright-field images will be discussed later in this paper.

4. Discussion

In our earlier study [14], a crystallographic mechanism for the transformation from α-Fe_2O_3 to Fe_3O_4 was proposed, using the rigid-sphere model. The mechanism can be summarized as follows;

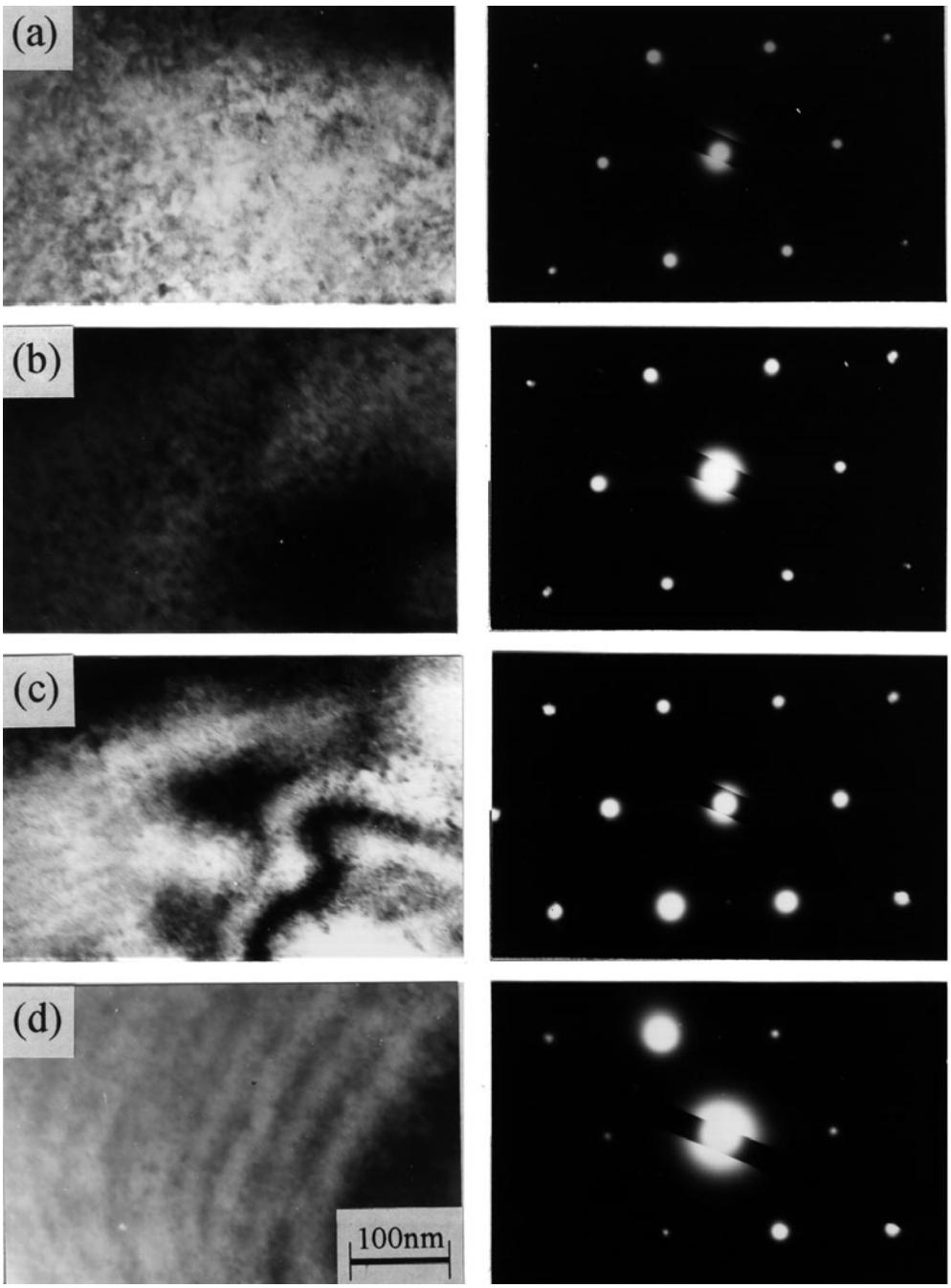

Figure 4. Results for the continuous observation of α-Fe_2O_3 implanted with 20 keV hydrogen ions at room temperature as a function of dose. (a) 4.9×10^{19} ions m^{-2}, (b) 4.13×10^{20} ions m^{-2}, (c) 1.07×10^{21} ions m^{-2} and (d) 2.26×10^{21} ions m^{-2}.

(1) The shear slipping occurs in every other $\{0001\}_h$ plane.
(2) The hcp-type stacking sequence of oxygen layers in α-Fe_2O_3 changes to the fcc-type stacking sequence of Fe_3O_4.

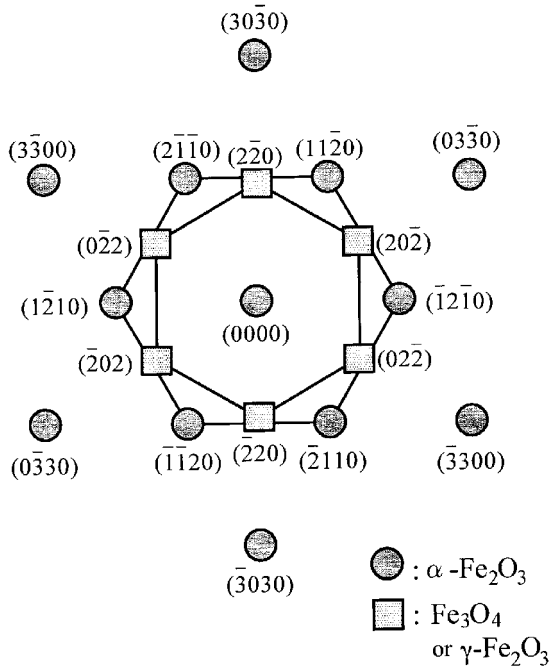

Figure 5. A schematic diffraction pattern consisting of a $[0001]_h$ pattern (●) and a $[111]_m$ pattern (■).

(3) While all of the iron ions in the α-Fe_2O_3 lattice are placed at octahedral sites (whose size is comparable to that of the iron ion), some of them in the re-stacked α-Fe_2O_3 lattice are placed at tetrahedral sites (whose size is much smaller than that of the octahedral site).
(4) The lattice is expanded by the re-stacking.
(5) The Coulomb force between iron ions and oxygen ions becomes weaker.
(6) Removal of the oxygen from the re-stacked α-Fe_2O_3 is induced by reaction with the reducing gas or implanted hydrogen.
(7) Some of the Fe^{3+} ions in the lattice turn into Fe^{2+} ions to maintain electroneutrality.
(8) The excess iron ions migrate to correct positions, resulting in an increase in the iron/oxygen ratio of the oxide.

On the other hand, the crystallographic mechanism of the transformation from α-Fe_2O_3 to γ-Fe_2O_3 can be summarized as follows [2]:

(1) The shear slipping occurs in every other $\{0001\}_h$ plane.
(2) The hcp-type stacking sequence of oxygen layers in α-Fe_2O_3 changes to the fcc-type stacking sequence of γ-Fe_2O_3.
(3) While all of the iron ions in the α-Fe_2O_3 lattice are placed at octahedral sites, some of them in the re-stacked α-Fe_2O_3 lattice are placed at tetrahedral sites.
(4) The lattice is expanded by the re-stacking.
(5) The iron ions migrate to correct positions.

These transformation mechanisms are summarized by an illustration shown as figure 6.

If these transformation mechanisms are correct and occur simultaneously, then the rapid lattice expansion should take place at the re-stacking stage. In this discussion, we will pay attention to the lattice constant changes during the hydrogen-ion implantation.

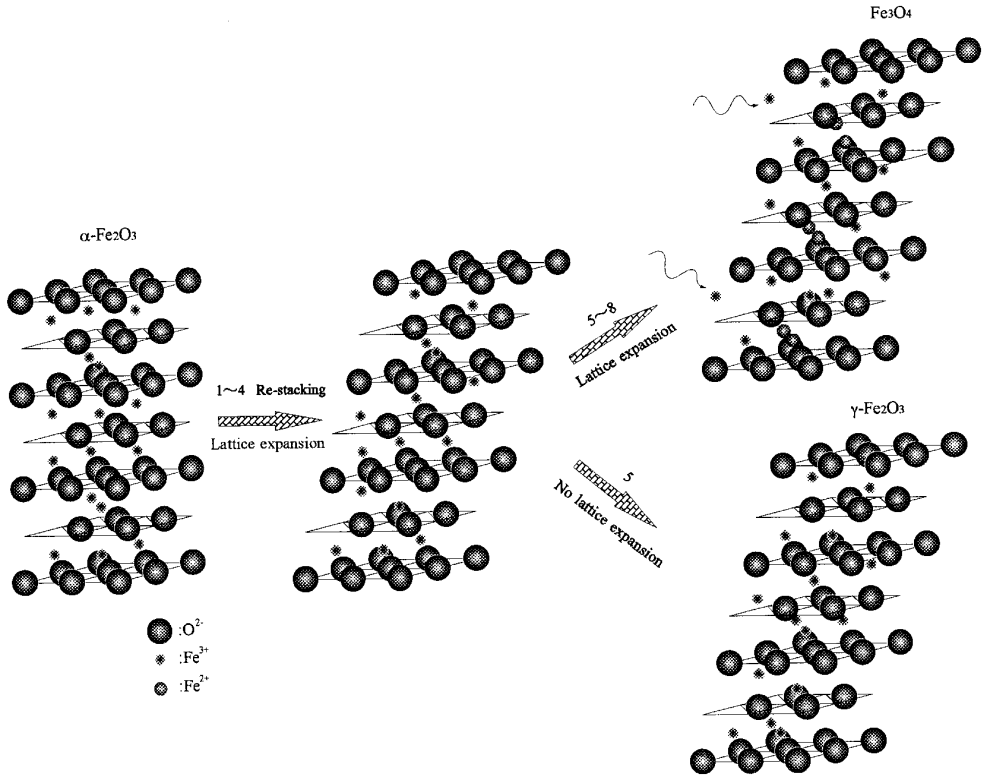

Figure 6. A summary of the crystallographic mechanisms of the transformations from α-Fe_2O_3 to Fe_3O_4 or γ-Fe_2O_3.

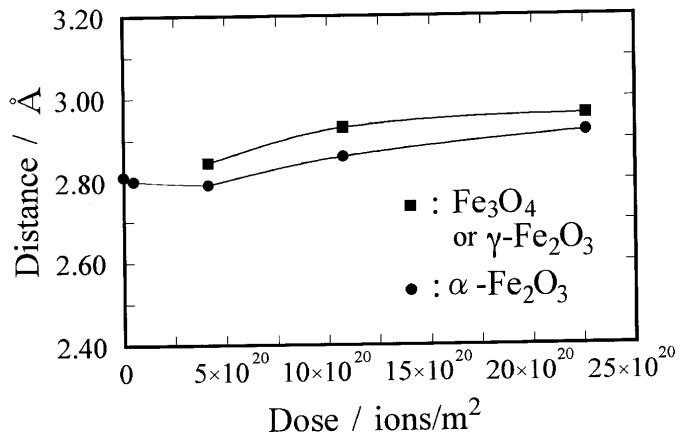

Figure 7. Changes of nearest interatomic distances of oxygen during the hydrogen-ion implantation.

Nearest interatomic distances of oxygen during the hydrogen-ion implantation are calculated from the diffraction patterns, and shown in figure 7. It is seen in this figure that the nearest interatomic distance does not vary upon implantation until the re-stacked phase appears at about 4.9×10^{19} ions m^{-2}. However, when the re-stacked phase is formed, the lattice

expansion is observed in the transformed (re-stacked) phase. In other words, the discontinuous lattice expansion occurs during the transformation from α-Fe_2O_3 to γ-Fe_2O_3 or Fe_3O_4. It is, therefore, found that the re-stacking results in instant lattice expansion, in agreement with both of the transformation mechanisms. Unfortunately, we cannot identify the hydrogen-ion-implantation-induced phase by using the above result.

After the formation of the re-stacked phase, it is found that the nearest interatomic distance of the re-stacked phase increases with dose. It is known that the hydrogen-ion implantation introduces many lattice defects, such as voids, dislocation loops and bubbles. However, since the lattice expansion was absent before the re-stacking, the main origin of the lattice expansion, after the re-stacking, cannot be attributed to the formation of these defects.

Next, we would like to discuss another possibility. If the hydrogen implantation causes a reduction from α-Fe_2O_3 to Fe_3O_4, then there should be Fe^{2+} ions in the implanted region. This is because, during the removal of the oxygen from the re-stacked phase, some of the Fe^{3+} ions in the lattice turn into Fe^{2+} ions to maintain electroneutrality, as shown in figure 6. It is known that the radius of an Fe^{2+} ion is 1.17 times larger than that of an Fe^{3+} ion. Moreover, the Coulomb force between the iron ion and the oxygen ion should become weaker because of the valence transition. Therefore, there is a possibility that the lattice expansion is caused by the removal of oxygen. In fact, the lattice constant of Fe_3O_4 (in which Fe^{2+} and Fe^{3+} ions coexist) is larger than that of γ-Fe_2O_3 (in which only Fe^{3+} ions coexist). In other words, the lattice expansion does not develop during the transformation from α-Fe_2O_3 to γ-Fe_2O_3 after the re-stacking, as shown in figure 6. Therefore, the phenomenon of the removal of the oxygen from the re-stacked phase can explain why the re-stacked phase is expanded by the hydrogen-ion implantation. In this way, the Fe_3O_4 phase provides a more likely explanation for the observations presented in this study.

It must be noted here that the nearest interatomic distance of the matrix phase, like that of the re-stacked phase, increases with dose after the formation of the re-stacked phase. Of course, no lattice expansion can be expected to be caused in the α-Fe_2O_3 matrix by the above transformation mechanism from α-Fe_2O_3 to Fe_3O_4 alone. It is known that the nearest interatomic distance of oxygen in a close-packed plane changes from 2.909 to 2.967 Å during the transformation from α-Fe_2O_3 to Fe_3O_4. In this study, Shoji–Nishiyama orientation relationships are observed between the α-Fe_2O_3 and the Fe_3O_4 phases. That is, the close-packed planes and directions in the two lattices are parallel. Therefore, lattice misfit strain appears near the interface. Hayes and Grieveson [21] thought that the misfit between α-Fe_2O_3 and Fe_3O_4 was accommodated by interfacial dislocations. However, if this is correct then the lattice expansion should not be observed in the α-Fe_2O_3 matrix. Moreover, development of secondary dislocations was not observed in the bright-field images during the hydrogen-ion implantation. In our previous study, a very fine Fe_3O_4 phase was observed in the α-Fe_2O_3 matrix, distributed uniformly, when hydrogen ions were implanted into the α-Fe_2O_3 [9]. Judging from these facts, we conclude that the following mechanism is operative.

At low doses, the very fine re-stacked phase is uniformly formed in the α-Fe_2O_3 matrix. The lattice of the re-stacked phase is expanded by the hydrogen-ion implantation due to the reduction. At the same time, the lattice parameter in the α-Fe_2O_3 matrix increases with the dose to maintain coherency with the re-stacked phase. If such coherency is considered, the experimental fact that no Fe_3O_4 phase was detected from the bright-field images can also be understood.

5. Conclusions

In this study, an *in situ* observation of α-Fe_2O_3 transformation has been performed using a dual-ion-beam accelerator interfaced with a TEM. The α-Fe_2O_3-to-Fe_3O_4 transformation

was observed during the hydrogen-ion implantation of α-Fe_2O_3. The orientation relationship between α-Fe_2O_3 and Fe_3O_4 is found to be

$$(0001)_h \parallel (111)_m, \qquad [100]_h \parallel [10]_m.$$

This is the Shoji–Nishiyama orientation relationship, in agreement with previous studies. It was also found that the re-stacking accompanies lattice expansion. These experimental results support the model for the α-Fe_2O_3-to-Fe_3O_4 transformation proposed by Watanabe and Ishii [14].

Acknowledgments

The authors wish to thank Mr S Takemura for the preparation of the TEM samples. One of the authors (YW) acknowledges the Kazato Research Foundation. Part of this study was supported by a Grant-in-Aid for COE Research (10CE2003) from the Ministry of Education, Culture, Sports, Science and Technology of Japan.

References

[1] Goldschmidt H J 1942 *J. Iron Steel Inst.* **CXLVI** 157
[2] Kachi S, Momiyama K and Shimizu S 1963 *J. Phys. Soc. Japan* **18** 106
[3] Meillon S, Dammak H, Flavin E and Pascard H 1995 *Phil. Mag. Lett.* **72** 105
[4] Porter J R and Swann P R 1977 *Ironmaking Steelmaking* **4** 300
[5] Rau M-F, Rieck D and Evans J W 1987 *Metall. Trans.* B **18** 257
[6] Verma S K, Raynaud G M and Rapp R A 1981 *Oxid. Met.* **15** 471
[7] Rapp R A 1984 *Metall. Trans.* A **15** 765
[8] Jungling T L and Rapp R A 1984 *Metall. Trans.* A **15** 2231
[9] Watanabe Y, Takemura S, Kashiwaya Y and Ishii K 1996 *J. Phys. D: Appl. Phys.* **29** 8
[10] Furuno S, Hojou K, Izui K, Kamigaki N and Kino T 1988 *J. Nucl. Mater.* **155–7** 1149
[11] Ohnuki S, Hidaka Y and Takahashi H 1991 *Ultramicroscopy* **39** 197
[12] Hamada S, Hojou K and Hishinuma A 1993 *J. Nucl. Mater.* **205** 219
[13] Ishikawa N and Furuya K 1994 *Ultramicroscopy* **56** 211
[14] Watanabe Y and Ishii K 1995 *Phys. Status Solidi* a **150** 673
[15] Biersack J P and Haggmark L G 1980 *Nucl. Instrum. Methods* **174** 257
[16] Blackman M and Kaye G 1960 *Proc. Phys. Soc.* **75** 364
[17] Finch G I and Sinha K P 1957 *Proc. R. Soc.* A **241** 1
[18] Mathieu F and Rousset A 1993 *Phil. Mag.* A **67** 533
[19] Shoji H 1931 *Z. Kristallogr.* **77** 381
[20] Nishiyama Z 1936 *Sci. Rep. Tohoku Imperial Univ. (1st Ser.)* **25** 79
[21] Hayes P C and Grieveson P 1981 *Metall. Trans.* B **12** 579